Electric Glue: Electrically Controlled Polymer-Surface Adhesion

Ann R. Fornof,*,[†] Matthias Erdmann,[†] Ralf David,[‡] and Hermann E. Gaub*,[†]

[†]Chair for Applied Physics and Center for Nanoscience, Ludwig-Maximilians University, Amalienstrasse 54, Munich, Germany 80799
[‡]Center for Integrated Protein Science Munich, Butenandtstrasse 5-13, Munich, Germany 81377

Ⓢ *Supporting Information*

ABSTRACT: Polymer-surface interactions provide a basis for nanoscale design and for understanding the fundamental chemistry and physics at these length scales. Controlling these interactions will provide the foundation for further manipulation, control, and measurement of single molecule processes. It is this direction of control over nanoscale polymer-surface interactions that we explore with electric glue. The adhesion between surfaces and single molecules is manipulated based on an externally controlled potential in electric glue.

KEYWORDS: Single-molecule force spectroscopy, polymers, atomic force microscopy, electrochemistry
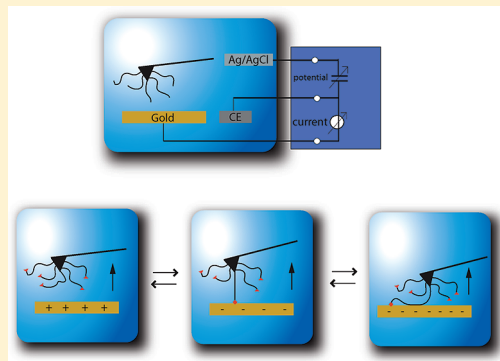
Electric potential has been used to attract polymers continuously to an electrode surface and to toggle molecules between states for a molecular switch.[2−4] For electric glue, the focus is to control the interaction of a polymer and an electrode surface reversibly, thus creating a nanoscale system with electrochemically controlled adhesion (Figure 1a). The reversible bonding of an organic molecule, DNA, to an inorganic surface, a gold electrode, was recently accomplished by varying the electric potential of the surface, and the interaction was measured via atomic force microscopy (AFM).[1] In the current work, control over electrosorption, or covalent bonding with the surface based on potential, is extended and refined to include physisorption, or noncovalent interaction between the polymer and the surface. The manipulation of the interaction and reaction of polymers from commercially available to tailored macromolecules with a surface is described.

To explore this concept further, we utilized a custom AFM setup with a working electrode as the surface of interest (Figure 1b). The polymers were covalently attached to the AFM tip and brought into contact with the surface of a gold working electrode at a specified potential. As the polymers were removed from the electrode in the z-direction, the resultant force was measured, and the potential of the electrode was changed by 10 mV. The potential of the electrode regulated oxidation/reduction reactions at the surface of the electrode.[5]

While the Au−S bond is the most studied bond for organic modification of gold surfaces, it has a bond strength close to that of the Au−Au bond.[6,7] Therefore, it is difficult to distinguish experimentally between Au−Au and Au−S bond rupture, and reversible attachment/detachment would be unpredictable due to the possibility of pulling gold nanowires from the surface of the electrode.[8] Therefore, the targeted bond for reversible

attachment was the dative, N−Au bond. The tip-attachment chemistry and polymeric chemistry were designed such that the N−Au bond was the weakest bond in the construct. For the N−Au reaction, the amine donates both electrons from its lone pair to share with undercoordinated gold in a classic example of a dative bond.[9,10]

Three polymers with differently charged backbones and primary amine end groups were utilized to control adhesion based on the electric potential of the surface, as well as to probe the influence of backbone charge on this process, in this series of experiments. Figure 1a depicts the experiment for the positively charged polymer. The same experimental setup was used for each of the experiments with polymers of differing backbone charge.

In each experiment, a different backbone charge on the polymer was explored by using an AFM tip functionalized with a different polymer. The neutral polymer chosen was poly-(ethylene glycol) (PEG-NH$_2$), a commercially available polymer; a 2,2-ionene, which was synthesized in-house (Supporting Information Figure S1), was selected for the positively charged backbone and finally, a biopolymer, double-stranded DNA, where three of the four bases contain primary amines, was used as the negatively charged polymer. Strong polyelectrolytes, whose charge in solution does not change substantially under moderate pH conditions, were chosen so that the polymeric backbone charge would remain the same at the bulk pH as well as the expected pHs local to the electrode surface.[11] A 2:1 electrolyte solution of 50 mM MgCl$_2$ at pH 8.5 provided an ambient for the dsDNA such that it would remain double-stranded and the
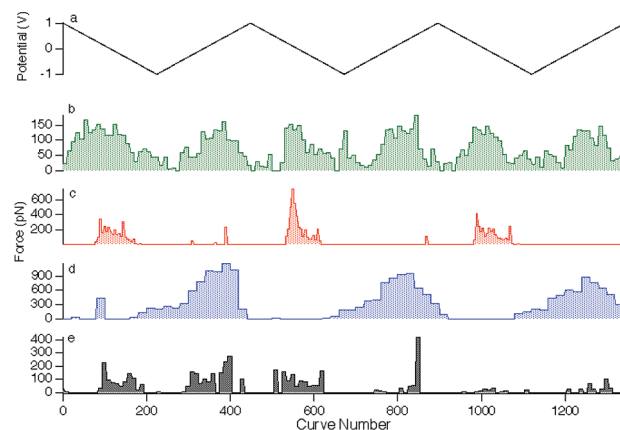
a)

b)
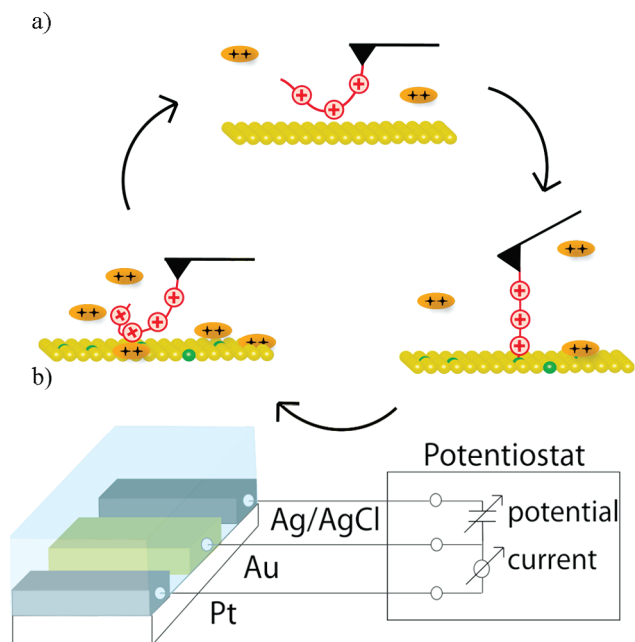
Figure 1. The experimental setup. (a) Throughout the electrochemical cycle from 1 to −1 V, the gold, working electrode surface undergoes oxidation and reduction and magnesium ions (shown in orange) from solution are attracted to the surface under certain potential ranges. The charged polymer responds to the surface chemistry of the electrode, ion concentration, and the availability of undercoordinated, reactive gold sites (shown in green). Under the appropriate conditions, the amine end group reacts with the gold surface, and the reactive surface is refreshed throughout the cycle, and the adhesion repeatedly occurs at the same potential ranges and is also turned off repeatedly. (b) The three electrode electrochemical cell used is comprised of a gold working electrode, a Ag/AgCl reference electrode, and a platinum counter electrode.

Figure 2. Rupture force with changing potential. (a) Potential was changed by 0.01 V with each force curve measured and was controlled by a potentiostat, force to rupture the amine−gold bonds plotted with the curve number (b) PEG-NH$_2$, (c) 2,2-ionene, (d) dsDNA (e) 2,2-ionene without MgCl$_2$; each of the curves were binned such that each bar represents ten force traces.

primary amines deprotonated. The same solution composition was utilized throughout the experiments with one exception. The no salt ionene experiment was performed without added MgCl$_2$.[12]

The neutral backbone of the PEG-NH$_2$ allowed for explicit examination of the N−Au bond. At static potential but varied loading rates, the force followed the expected behavior for covalent bond rupture (Supporting Information Figure S2).[13] The stretching of the polymer chain prior to rupture observed in the force curves indicated that the polymer was pinned at its end group (Supporting Information Figure S3).[14,15] Control experiments with PEG and a methoxy end group showed no interaction between the polymer and the surface (data not shown).

Under dynamic potential, the force to remove the polymer from the surface was determined as the potential was cycled from 1 to −1 V via an externally controlled potentiostat (Figure 2a). The change in potential is shown in Figure 2a, and the rupture force under those potential conditions is shown in Figure 2b−e. After each force curve, the potential was changed by 0.01 V and a curve number assigned to the force curve at that potential. The data in the graph was binned such that each bar in the graph represents ten force curves. Because of the binning of the data, the absolute forces measured can reflect in part the likelihood of a successful N−Au bonding event. A high-tip functionalization density was used to prolong the longevity of the experiment.

Over several hundred or thousand force curves the functionalization of the tip was observed to decrease (see, for example, Figure 2e); this tip wear-out may have been due to mechanical damage to the tip over these long experiments. However, the last rupture event in the force curve was measured, and thus, only single polymer events were recorded. The small potential steps minimized artifacts due to ion currents acting on the cantilever.

The data is plotted in a roburogram (robur is Latin for force), where the rupture force is plotted versus potential. This plot is akin to the cyclic voltammogram (Figure 3a) except that the y-axis is the rupture force rather than current (Figure 3b−d). The adhesion of PEG-NH$_2$ was reduced at the highest and lowest potential regimes explored and was only moderately sensitive to the direction of charging as indicated by the slight hysteresis in the roburogram at potentials around 0.3 to 0.5 V (Figure 3b). Near the potential extremes (1 or −1 V), there was negligible interaction between the polymer and the surface. The reversible electrosorption of PEG-NH$_2$ was observed for over 2000 force curves; thus demonstrating the longevity and reproducibility of the adsorption (Supporting Information Figure S4).

The PEG-NH$_2$ provided a baseline for the behavior of the N−Au reaction and demonstrated the control possible over electrosorption of the N−Au bond based on the applied potential to the surface. The polymers could then be tailored to exert control over the physisorption through the introduction of charge to the polymer backbone in combination with electrosorption due to the coordinate N−Au bond.

Rather than the polymer interacting with the electrode under all potential conditions except at the extreme potentials, as was the case for PEG-NH$_2$, the amine-end-capped ionene with its positively charged backbone began reacting with the surface at potentials close to 0.3 V only when the potential was ramped down from 1 V. However, there was negligible interaction between the polymer and the working electrode surface in the reverse direction (Figure 3d).

A strong hysteresis was also observed for the potential-dependent interaction of dsDNA with the gold electrode. Three of the four nucleotides that are found in DNA contain primary amine functionality, that is, adenine, guanine, and cytosine; only thymine does not have a primary amine moiety (Supporting
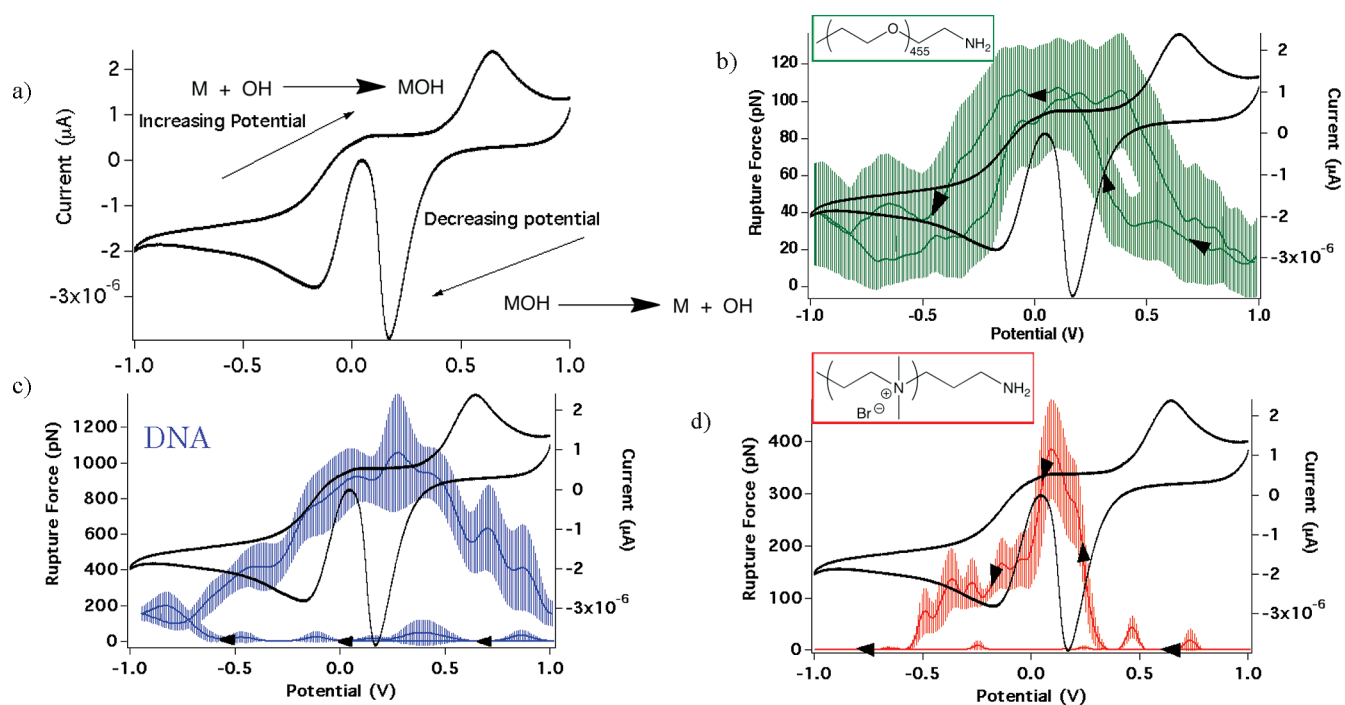
Figure 3. Voltammogram of the gold electrode overlaid with the roburograms (roburo from force in Latin) for each of the polymers. The black arrows on the roburograms indicate decreasing potential. (a) Peaks in the voltammogram of the gold electrode performed at a sweep rate of 0.1 V/s show oxidation when increasing potential and reduction during decreasing potential; (b) PEG-NH$_2$ reacted with the gold surface under potentials of 0.5 to −0.5 V and showed virtually no hysteresis; (c) DNA with amine-containing nucleotides interacted with the electrode when the potential was reduced from −0.6 to −1 V and continued to interact as the potential was increased from −1 to 1 V. The interaction of dsDNA with the electrode began to fall off when the gold surface started to oxidize and thus become less reactive. (d) 2,2-Ionene showed significant hysteresis and reacted with the gold surface after the gold reduction until about −0.5 V when decreasing potential. The data was smoothed.

Information Figure S5). Double-stranded DNA is known to be "frayed" at the end exposing the typically interior base pairs at room temperature.[16] dsDNA with a random nucleotide sequence except for the final five bases was utilized in these experiments. The last five nucleotides were adenines and on the complementary strand, thymines. The same DNA strand was covalently attached to the AFM tip on the opposite end as the adenine groups of that strand. Thus, when the bond rupture occurred between the primary amines of the adenines and the gold surface, the weakest bond was the N—Au bond. However, had the construct been reversed and the strand with thymine end groups covalently attached to the tip, the strand with adenine and therefore N—Au bonds would have melted away from the thymine end-capped strand and remain at the gold surface.[1]

Several factors dictate the bonding of polymers to the electrode. One factor appears to be the noncovalent influence of backbone charge. The two polymers with charged backbones show a strong hysteresis and indeed a virtually mirror image of the reactivity with the gold surface as demonstrated by their roburograms despite both having primary amine end groups (Figure 3c,d). However, the impact of backbone charge is somewhat counterintuitive. The dsDNA with its negatively charged backbone begins interacting with the gold surface at the most negative potentials whereas the ionene interacted with the surface at negative potentials but only in one direction of applied potential.

However, the polymers are not the only charged species in solution. The MgCl$_2$, which was added to the solution to help

stabilize the dsDNA double helix, can diffuse to and accumulate at the surface of the electrode. To address the memory effect observed for the oppositely charged polymers, the Langmuir adsorption isotherm was calculated of MgCl$_2$ and showed the adsorption of Mg^{2+} at the electrode surface.[17] As the applied potential was brought from 0 V through −1 V and back to 0 V, Mg^{2+} ions accumulated at the surface of the electrode as determined by the adsorption isotherm (Supporting Information Figure S6). While experiments without added salt for dsDNA were not possible due to the destabilization of the double helix, the behavior of the ionene without added salt was similar to that of PEG-NH$_2$ (Figure 2e). No hysteresis was observed in the roburogram for the ionene when there was no Mg^{2+} to accumulate at the electrode surface.

The calculation of Mg^{2+} accumulation at the surface of the electrode and the behavior of the ionene without Mg^{2+} in solution indicated that the interaction between the positively charged backbone of the ionene and Mg^{2+} was responsible for the hysteresis observed in the roburogram of the ionene (Figure 3d). The positively charged backbone of the ionene was repulsed by the doubly charged, positive magnesium ions at the surface further restricting the interaction of the polymer with the gold surface as demonstrated by the lack of interaction observed from −1 to 0 V. Also, in the case of DNA the divalent, cationic Mg^{2+} can mediate between the negatively charged backbone of DNA and the surface, which has also been observed in DNA—mica interactions.[18−25] Once at the electrode surface, the dsDNA could find a gold reactive site.

Another factor controlling electric glue behavior is the oxidation state of the gold electrode itself. As noted earlier, the PEG-NH_2 polymer gives us the opportunity to explore the influence of the N—Au bond explicitly without the complication of backbone charge. It also gives the first indication of when the gold electrode is reactive. The PEG-NH_2 reacted with the gold electrode only when the gold was reduced as indicated by the onset of reaction when decreasing potential (at ∼0.3 V), which coincides with gold reduction. During the increasing potential sweep, the reaction subsided once the gold surface was again oxidized. The reactive gold sites are occupied with a hydroxide monolayer (∼0.8 to 0.3 V) when the electrode is oxidized. In the reduced state, the gold atoms are again available and free to react with the amine end groups (∼0.3 to 0.8 V; Figure 3a).

The dsDNA and ionene only react with the surface when it is reduced and the directionality of interaction was determined by the inclusion of salt. As shown in Figure 3b—d, as soon as the gold is oxidized, the polymers no longer bond to the surface, as the possible reactive sites are otherwise occupied. In the case of dsDNA, the bonding subsides when the gold surface is oxidized when increasing potential at approximately 0.8 V (Figure 3c) and resumes once the surface is sufficiently reduced to accommodate N—Au bonding as described in Erdmann et al.[1] This explains the absence of bonding from approximately 0.8 V during the increasing potential sweep for the dsDNA. As soon as the electrode was cycled through the positive potentials and brought to low enough potentials, where reduction occurred and a bare metal surface was regenerated (∼0.3 V), the 2,2-ionene began interacting with the surface again (Figure 3d). PEG-NH_2 and ionene do not react with the gold electrode under the most negative potentials. It is likely that at the most negative potentials the undercoordinated gold atoms are more satisfied with electrons rendering them less reactive. As the dsDNA has more reactive groups from the multiple nucleotides and is longer than both the PEG-NH_2 and ionene, the dsDNA could thermally scan more of the surface, making it more likely for the dsDNA to find a reactive gold site despite the lower reactivity of the surface.

The maximum rupture forces for the polymers that we used as electric glue differed substantially. The maximum rupture forces for the dsDNA exceeded 800 pN while the maximum rupture forces for the PEG-NH_2 hovered around 150 pN (Figure 2b—e). The dsDNA experiment was unique in that it was possible that more than one amine per polymeric chain to react with the surface. This contributed to the dsDNA having the highest rupture forces, where more than one nucleotide on the same chain could rupture simultaneously. And as noted earlier, the binning of the data meant that the absolute rupture force values can also reflect the frequency of bonding and not just absolute bond rupture force.

Covalent attachment of a polymer to a metal surface was electrically modulated. Electrochemical control was demonstrated not only for biopolymers but also for commercially available and synthetic polymers. The adhesion was tuned by the addition of backbone charge to the polymer such that the polymer end group reacted with the surface or not based on the direction of applied potential. The polymers also provide an ultrasensitive indicator of the electrochemistry occurring at the electrode surface.

ASSOCIATED CONTENT

S **Supporting Information.** Additional information and figures. This material is available free of charge via the Internet at http://pubs.acs.org.

AUTHOR INFORMATION

Corresponding Author

*E-mail: (A.R.F.) ann.fornof@physik.uni-muenchen.de; (H.E.G.) gaub@lmu.de.

REFERENCES

(1) Erdmann, M.; David, R.; Fornof, A. R.; Gaub, H. E. *Nature Chem.* **2010**, *2*, 745.

(2) Erdmann, M.; David, R.; Fornof, A. R.; Gaub, H. E. *Nature Nanotechnol.* **2009**, *5*, 154.

(3) Ngankam, A. P.; Van Tassel, P. R. *Proc. Natl. Acad. Sci. U.S.A.* **2007**, *104*, 1140.

(4) Collier, C. P.; Wong, E. W.; Belohradsky, M.; Raymo, F. M.; Stoddart, J. F.; Kuekes, P. J.; Williams, R. S.; Heath, J. R. *Science* **2007**, *285*, 391.

(5) Hamelin, A.; Sottomayor, M. J.; Silva, F.; Chang, S. C.; Weaver, M. J. *J. Electroanal. Chem.* **1990**, *295*, 291.

(6) Krüger, D.; Fuchs, H.; Rousseau, R.; Marx, D.; Parrinello, M. *Phys. Rev. Lett.* **2002**, *89*, 186402.

(7) Li, Z.; Kosov, D. S. *Phys. Rev. B* **2007**, *76*, 035415.

(8) Grandbois, M.; Beyer, M.; Rief, M.; Clausen-Schaumann, H.; Gaub, H. E. *Science* **1999**, *283*, 1727.

(9) Venkataraman, L.; Klare, J. E.; Tam, I. W.; Nuckolls, C.; Hybertsen, M. S.; Steigerwald, M. L. *Nano Lett.* **2006**, *6*, 458.

(10) Quek, S. Y.; Venkataraman, L.; Choi, H. J.; Louie, S. G.; Hybertsen, M. S.; Neaton, J. B. *Nano Lett.* **2007**, *7*, 3477.

(11) Hessami, S.; Tobias, C. W. *AIChE J.* **1993**, *39*, 149.

(12) Wenner, J. R.; Williams, M. C.; Rouzina, I.; Bloomfield, V. A. *Biophys. J.* **2002**, *82*, 3160.

(13) Clausen-Schaumann, H.; Rief, M.; Tolksdorf, C.; Gaub, H. E. *Biophys. J.* **2000**, *78*, 1997.

(14) Oesterhelt, F.; Rief, M.; Gaub, H. E. *New Journal of Physics* **1999**, *1*, 10.1088/1367.

(15) Guzman, D. L.; Randall, A.; Baldi, P.; Guan, Z. *Proc. Natl. Acad. Sci. U.S.A.* **2010**, *107*, 1989.

(16) Andreatta, D.; Sen, S.; Lustres, J. L.; Kovalenko, S. A.; Ernsting, N. P.; Murphy, c. j.; Coleman, R. S.; Berg, M. A. *J. Am. Chem. Soc.* **2006**, *128*, 6885.

(17) Duval, J.; Lyklema, J.; Kleijn, J. M.; van Leeuwen, H. P. *Langmuir* **2001**, *17*, 7573.

(18) Hansma, H. G.; Vesenka, J.; Siegerist, C.; Kelderman, G.; Morrett, H.; Sinsheimer, R. L.; Elings, V.; Bustamante, C.; Hansma, P. K. *Science* **1992**, *256*, 1180.

(19) Rothemund, P. W. K. *Nature* **2006**, *440*, 297.

(20) Ruiz, R.; Kang, H.; Detcheverry, F. A.; Dobisz, E.; Kercher, D. S.; Albrecht, T. R.; de Pablo, J. J.; Nealey, P. F. *Science* **2008**, *321*, 936.

(21) Han, E.; Stuen, K. O.; La, Y.-H.; Nealey, P. F.; Gopalan, P. *Macromolecules* **2008**, *41*, 9090.

(22) Hung, A. M.; Micheel, C. M.; Bozano, L. D.; Osterbur, L. W.; Wallraff, G. M.; Cha, J. N. *Nat. Nanotechnol.* **2009**, *5*, 121.

(23) Seeman, N. C. *Nature* **2003**, *421*, 427.

(24) Kufer, S. K.; Puchner, E. M.; Gumpp, H.; Liedl, T.; Gaub, H. E. *Science* **2008**, *319*, 594.

(25) Maune, H. T.; Han, S.-p.; Barish, R. D.; Bockrath, M.; Goddard, W. A., III; Rothemund, P. W. K.; Winfree, E. *Nature Nanotechnol.* **2009**, *5*, 61.